

UCC Library and UCC researchers have made this item openly available. Please [let us know](#) how this has helped you. Thanks!

Title	Reinventing solid state electronics: harnessing quantum confinement in bismuth thin films
Author(s)	Gity, Farzan; Ansari, Lida; Lanius, Martin; Schüffelgen, Peter; Mussler, Gregor; Grützmacher, Detlev; Greer, James C.
Publication date	2017-03-03
Original citation	Gity, F., Ansari, L., Lanius, M., Schüffelgen, P., Mussler, G., Grützmacher, D. and Greer, J. C. (2017) 'Reinventing solid state electronics: harnessing quantum confinement in bismuth thin films', Applied Physics Letters, 110(9), 093111 (5pp). doi:10.1063/1.4977431
Type of publication	Article (peer-reviewed)
Link to publisher's version	ftp://ftp.aip.org/epaps/appl_phys_lett/E-APPLAB-110-027709 http://dx.doi.org/10.1063/1.4977431 Access to the full text of the published version may require a subscription.
Rights	© 2017, the Authors. Published by AIP Publishing. This article may be downloaded for personal use only. Any other use requires prior permission of the authors and AIP Publishing. The following article appeared in F. Gity et al., Applied Physics Letters, 110(9), 093111 (5pp) and may be found at http://dx.doi.org/10.1063/1.4977431
Item downloaded from	http://hdl.handle.net/10468/5728

Downloaded on 2019-04-22T23:57:49Z

Supporting Material for

Reinventing Solid State Electronics: Harnessing Quantum Confinement in Bismuth Thin Films

Farzan Gity¹, Lida Ansari¹, Martin Lanius², Peter Schüffelgen², Gregor Mussler²,
Detlev Grützmacher², James C. Greer^{1*}

¹ Tyndall National Institute, Lee Maltings, Dyke Parade, Cork, Ireland T12 R5CP

² Peter Grünberg Institute 9 & Jülich Aachen Research Alliance (JARA-FIT), Research Center Jülich, Germany

Email: *Jim.Greer@tyndall.ie

Materials and Methods

Bismuth thin films were grown by molecular beam epitaxy (MBE) on Si(111) wafers. X-ray reflectivity (XRR) measurements for three exemplary Bi layers are displayed in Fig. S1(A) whereas Fig. S1(B) shows the results from X-ray diffraction (XRD) measurements for the same set of thin films. The high-resolution cross-sectional transmission electron microscopy (HR-XTEM) image of the 5.7 nm film is shown in Fig. S1(C) and is consistent with the single crystal nature of the bismuth thin films.

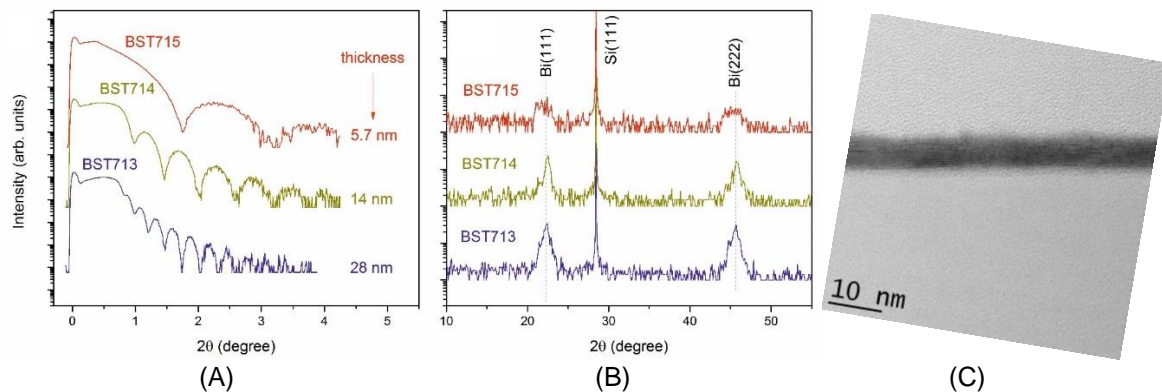


Fig. S1 - (A) XRR of bismuth film with thicknesses of 5.7 nm, 14 nm and 28 nm on Si (111). (B) XRD of 5.7 nm, 14 nm and 28 nm bismuth film thicknesses on Si (111). (C) HR-XTEM of 5.7 nm Bi film grown by MBE on Si(111).

Supplementary Text

Computational details - The norm-conserving pseudopotentials utilizing the Perdew-Zunger form of local density approximation (LDA) are used in the density functional theory (DFT) calculations [S1]. For the numerical atomic orbital basis set [S2], three orbitals per atomic level are defined with the cutoff distance of 7 Bohr. The atomistic structure is relaxed with respect to atom positions and the simulation cell parameters to minimize the total energy such that the maximum force component per atom is less than 0.01 eV/Å. It is well known that commonly applied approximations such as LDA to the exchange correlation functional in DFT underestimate band gaps in semiconductors and insulators. Electronic structure using DFT can allow for a characterization of a wide variety of materials as conductors, semiconductors, or metals. However, to provide a quantitative description of the opening of a band gap in bismuth nanowires due to quantum confinement requires a more accurate treatment of the band structure. The *GW* (*G*: Green's function, *W*: screened Coulomb interaction) approximation is a method for determining quasi-particle excitations in many-electron systems and provides an accurate prediction of band gaps that are in good agreement with experimental values [S3]. The *GW* method has the advantage of providing accurate band gap estimates without empirical corrections, whereas other DFT methods such as hybrid functionals and DFT corrected using the Hubbard-*U* parameter typically use the band gap for calibration. However we note recent progress with Hubbard-*U* corrected DFT and meta-GGA functionals that can eliminate empiricism in the calculation of band gaps and with increased computational efficiency. In the main text, the effects of band gap widening due to quantum confinement are described using the *GW* approximation. In the following, the DFT calculations are detailed to provide information on the simulation cells used for the calculations and to provide information on the geometry of atomistic models for thin films, details of their density of states (DoS), and the effect of surface termination on thin bismuth films.

The MBE Bi films' orientation in the growth direction is trigonal. To investigate the influence of quantum confinement on the emergence of a band gap in bismuth thin films of varying thicknesses with trigonal orientation normal to the surface, electronic structure calculations for bismuth slab models of approximately 2 nm Bi thickness are performed. Fig. S2(A) and Fig. S2(B) show side views of slabs with hydroxyl (–OH) surface termination and without surface terminations for the relaxed structures. Top views of the slabs are shown in Fig. S2(C). The bilayers characteristic of bulk bismuth in the [111] orientation form covalently bonded layers normal to the surface. The atoms' next-nearest neighbors are in adjacent bilayers and bonding within a bilayer is much stronger than the inter-bilayer bonding. The slab model without surface termination shows a ~3% reduction in the next-nearest neighbors' bonds lengths compared to the bulk Bi structure. The reduction for the slab model with –OH terminating group increases by ~6% while the nearest neighbor bond length is not modified significantly either with or without surface hydroxyl groups. The charge difference distribution in lateral plane is shown for the Bi thin film with –OH and without termination in Fig. S2(D) and S2(E), respectively. The blue coloring indicates charge accumulation and red coloring indicates charge depletion relative to neutral atomic charge densities providing an indication of the charge reorganization occurring in the slabs for bond formation. Due to the electronegativity of –

OH, there is a considerable charge transfer to the surface for the passivated slab model. The impact of stronger surface charge transfer on the formation of a band gap in the $-OH$ passivated slab is shown in Fig. S2(E) in which the DoS of the $-OH$ terminated slab is compared with the DoS for the slab without termination and hence in the presence of surface dangling bonds. The projected DoS (PDoS) for Bi atoms located at the surface and core of the Bi slab model with and without surface passivation is plotted in Fig. S2(F). As illustrated, the PDoS of atoms near the surface of the unpassivated slab varies significantly in comparison to core atoms for energies about the Fermi level. Within the $-OH$ terminated slab model, there is not a significant difference in the PDoS between the surface and core metal atoms revealing the elimination of the surface dangling bonds.

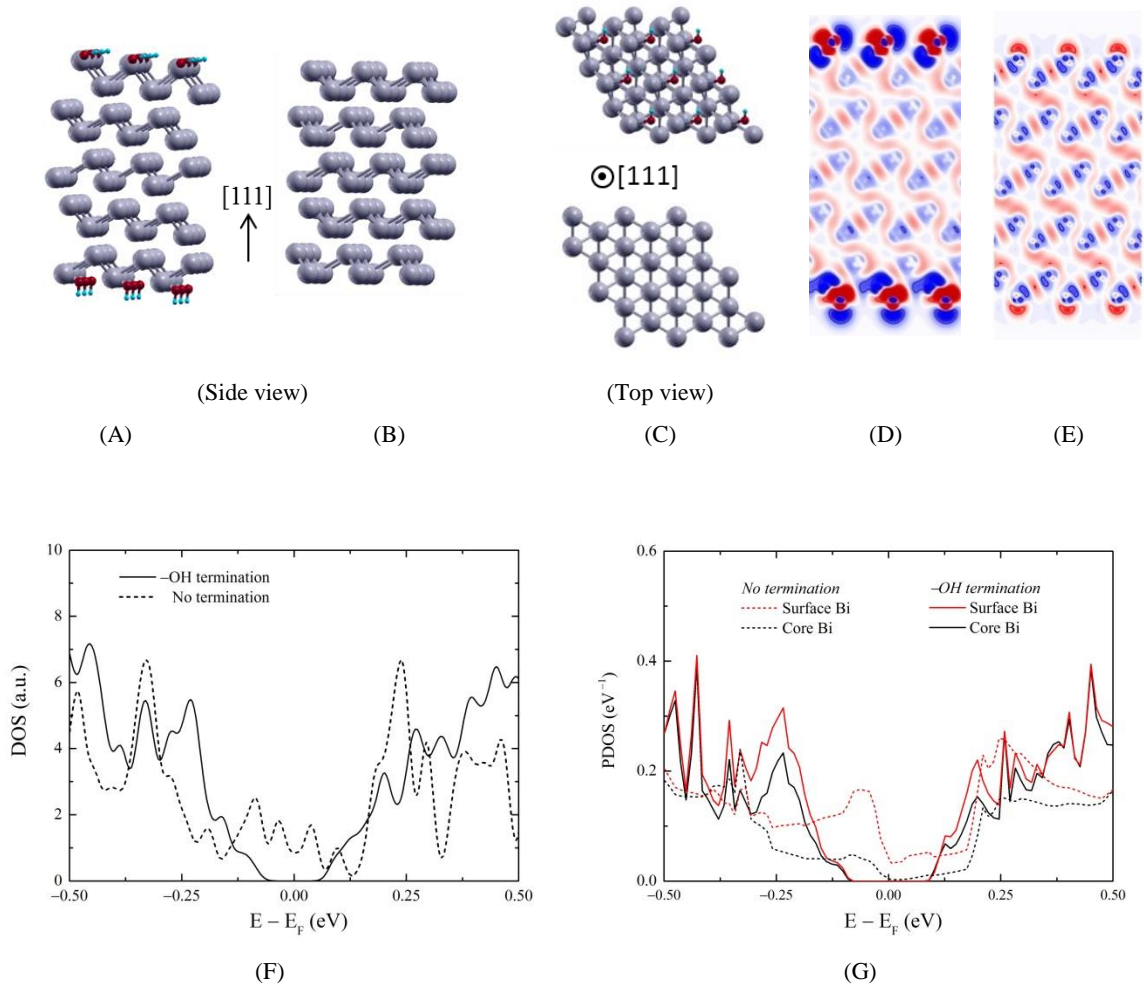


Fig. S2 - Atomic illustration of relaxed (strain free) Bi slab models. Side view (A) with hydroxyl surface termination, and (B) without surface termination. Top view with hydroxyl (C-top) and without (C-bottom). Contour plot of lateral plane charge difference density distributions for Bi slabs for (D) hydroxyl surface termination, and (E) without. (F) Total DoS for the Bi thin films with $-OH$ termination and without. (G) PDoS for surface and core Bi atoms with and without $-OH$ termination.

The DoS of the etched 8nm, 4nm, and 1.5nm films (*i.e.*,) is compared to the as-grown 12 nm film illustrated in Fig. S3. The band gap in thin region emerges and increases as the thickness of the film decreases. We note that the electronic structure of the thin films is sensitive to the surface passivation scheme, and that there is a relatively small energy difference for alternative –OH bonding structures which lead to metallic surface states. This suggest that passivation of the (111) surface requires a sharp interface and well defined oxide bonding.

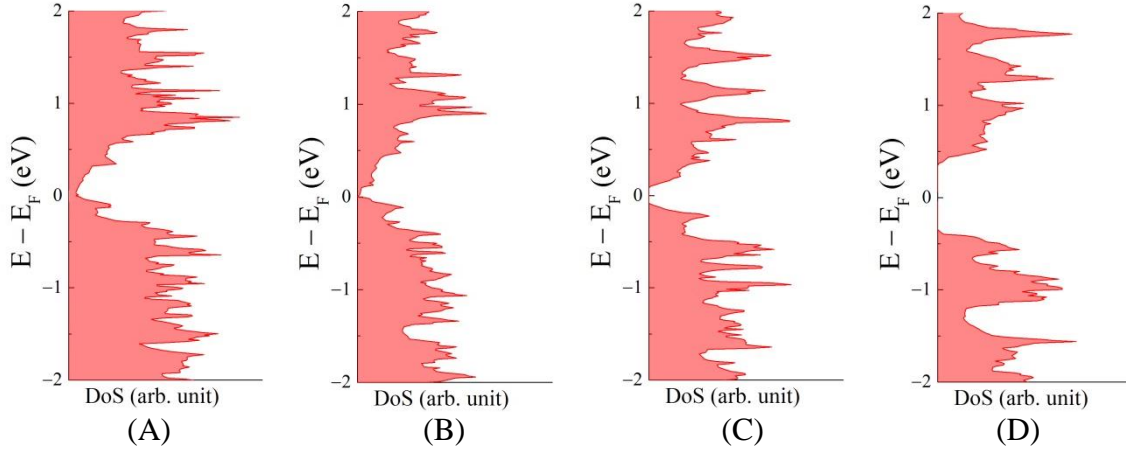


Fig. S3 – The density of states for bismuth bulk and thin films from DFT calculations corresponding to schematic band structures shown in Fig. 3 of the main text for simulation slabs of thickness (A) bulk, (B) 8 nm, (C) 4 nm, and (D) 1.5 nm with hydroxyl termination.

Electrical characterization details - Electrical measurements of the circular transmission line model (cTLM) contacts on the 12 nm un-etched sample (reference sample) show Ohmic current-voltage (IV) characteristics as presented in Fig. S4.

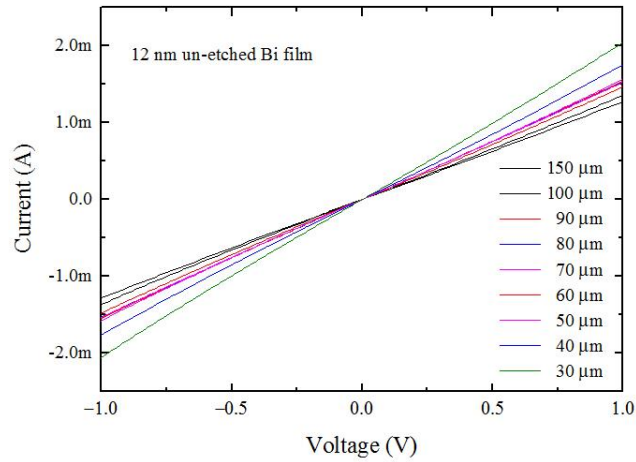


Fig. S4 - Electrical measurements of the cTLM contacts on the 12 nm un-etched sample (reference sample) showing Ohmic current-voltage (IV) characteristics.

Current-voltage (IV) characteristic of the 12nm/1.5nm diode at room temperature is shown in Fig. S5 corrected for the effect of the series resistance (R_s). R_s and ideality factor of the diode is extracted by fitting the measured data with the diode equation. Including a series resistance of $\sim 150 \text{ k}\Omega$ to describe the contact resistance due to the presence of Bi native oxide at the interface of the thick Bi section of the junction and metal contact. With an ideality factor of 1.82, the forward current characteristic is well described as an exponential function of applied voltage bias across the junction.

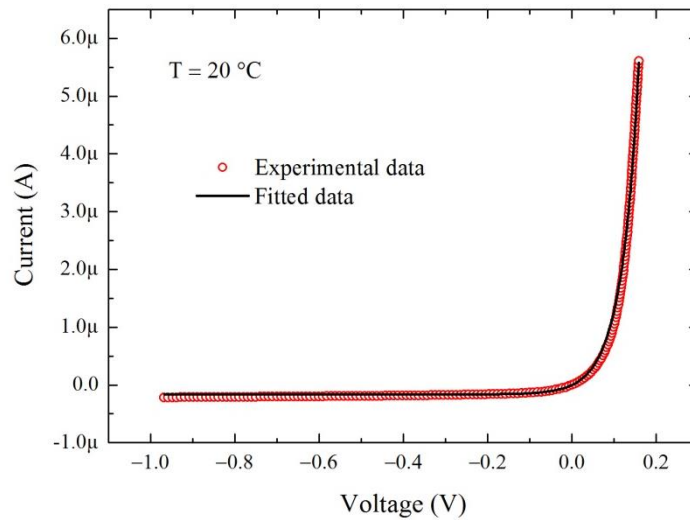


Fig. S5 - Current-voltage (IV) characteristic of the *homomaterial* bismuth junction formed with film thicknesses 12nm/1.5nm operating near room temperature with the effects of parasitic series resistance of 150 k Ω removed.

Finally, in Fig. S6 the current-voltage characteristic is for the 12nm/4nm junction is shown measured at T=-40 °C. The junction becomes rectifying at lower temperatures consist with a smaller voltage barrier for the 12nm/4nm film relative to the 12nm/1.5nm junction. The 12nm/8nm film remains Ohmic for all temperatures greater than -40 °C consistent with a voltage barrier comparable to $k_B T$ at room temperature.

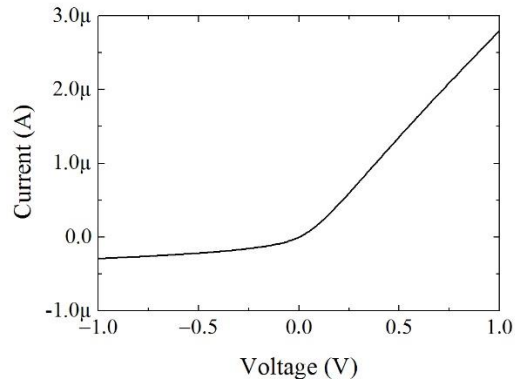


Fig. S6 – Current voltage characteristic for the 12nm/4nm junction at T=-40 °C. The same junction is nearly Ohmic at T=+20 °C consistent with a smaller voltage barrier relative to the 12nm/1.5nm junction.

References

- S1. Perdew, J.P.; Zunger, A. *Phys. Rev. B* **1981**, 23, 5048 – 5079.
- S2. Ozaki, T.; Kino, H. *Phys. Rev. B* **2004**, 69, 195113-1 – 195113-19.
- S3. Schilfgaarde, M.V.; Kotani, T.; Faleev, S. *Phys. Rev. Lett.* **2006**, 96, 226402-1 – 226402-4.